

# LC Scintillator-based Muon Detector/Tail-catcher R&D

R. Abrams<sup>1</sup>, G. Blazey<sup>2</sup>, A. Driutti<sup>6</sup>, A. Dychkant<sup>2</sup>, H.E. Fisk<sup>3</sup>, A. Gutierrez<sup>4</sup>, P. Karchin<sup>4</sup>,  
M. McKenna<sup>5</sup>, C. Milstene<sup>3</sup>, A. Para<sup>3</sup>, G. Pauletta<sup>6</sup>, R. Van Kooten<sup>1</sup>, M. Wayne<sup>5</sup>, V. Zutshi<sup>2</sup>

1 – Department of Physics, Indiana University, Bloomington, IN 47405, U.S.A.

2 – Department of Physics, Northern Illinois University, DeKalb IL 60115, U.S.A.

3 – Fermilab, P.O. Box 500, Batavia, IL 60510, U.S.A.

4 – Department of Physics and Astronomy, Wayne State University, Detroit MI 48201, U.S.A.

5 – Department of Physics, University of Notre Dame, Notre Dame, IN 46556, U.S.A.

6 – Università di Udine 33100 Udine, UD Italy

Preliminary analysis of test beam data from strip scintillator planes read-out with multi-anode PMTs (MAPMTs) is presented along with a description of the independent systematic measurements of relative response for all channels of several MAPMTs used in the tests. Test beam measurements for the response of a scintillator strip, read out with Si photo-sensors, is also described.

## 1 Introduction

This report[1] describes tests of four 2.5 m X 1.25 m area ILC pre-prototype strip-scintillator planes exposed to a +120 GeV/c hadron beam in the Meson area at Fermilab. The objectives of the tests were to measure the response of the strip scintillator (1cm thick X 4.1cm wide) equipped with a 1.2 mm diameter green light collecting wavelength shifting (WLS) fiber glued in a longitudinal channel along the length of the strip. For readout purposes the WLS fiber was thermally fused to a clear fiber of the same diameter near the exit of the strip to transmit light pulses, generated by charged hadrons, to the multi-anode photo-multiplier that was used to convert the light pulses to signals that were then digitized.

The parallel strip-scintillator that makes up the planes is oriented at  $\pm 45^\circ$  relative to the boundaries of each plane. Two of the four planes had a single clear fiber per strip to carry the light to its photo-sensor. These planes are labeled S+ and S- to indicate single-ended readout strips.

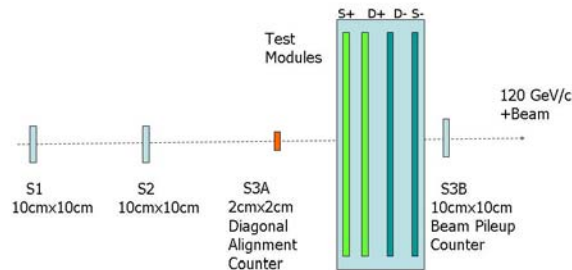


**Figure 1: MTest beam setup of four planes of scintillator strips and the beam defining counters.**

The other two planes have clear fibers fused to each end of the WLS fiber to provide dual paths for light to reach two photo-sensors. These two planes are labeled D+ and D-. The two ends of each D-plane fiber are labeled D(a) or D(b). Each plane has 22 full length strips (1.87 m) and 42 partial length strips, 21 to fill each of the two corners of a given plane. This geometry is chosen to limit the maximum length of scintillator bars, WLS fibers and consequent attenuation of scintillator generated light and the possible need for double-ended readout.

## 2 Test-beam Set-up

Figure 1 shows schematically the four planes of strips and beam defining counters. The MTest (primary) proton beam was approximately 1 cm FWHM in diameter. The 2 cm X 2 cm S3A counter was mounted diagonally to define the fixed beam position. The four planes were mounted on a movable cart so they could be positioned vertically and horizontally to put beam through one strip in each plane. The beam trigger required a four-fold coincidence of the counters as indicated in Fig. 1. The pulse height for S3B was digitized for use in the analysis to veto multiple beam particles during the ADC gate.

The 64 channel multi-anode PMTs, Hamamatsu 7546B run at 970 V, were used to convert light to electrical signals. The anode signals passed via a special printed circuit board from the MAPMT base to paddle cards that separated the output from 16 channels into RG-174 coaxial cable that terminated at a patch panel. From there RG-58 cables carried the signals to LeCroy X10 amplifiers where they were split and delayed for timing purposes before they entered LeCroy 2249A ADCs. The LRS 2249A's digitized the delayed signals that were contained in an ADC gate that was triggered by the four-fold beam coincidence. The ADC gate was 170ns to accommodate signals from any of the instrumented strips. The digitized ADC outputs were readout with a standard CAMAC system at a rate that was restricted to about 50 Hz. When we were the prime user we had low intensity beam,  $\sim 1000$  p/sec, two 1 s spills per minute, 12 hours per day. Ten percent of the ADC gates contained additional beam particles, even at low rates. This fraction was measured by digitizing the output of the SC3B counter for all recorded beam triggers. During the data analysis events, with a pulse height in SC3B that was more than a single minimum ionizing particle, were rejected from further analysis.

There were a total of 384 channels associated with the MAPMTs. Due to our limited DAQ rate we used a total of slightly less than 40 ADC channels. Each LRS 2249A ADC channel was separately calibrated. The nominal calibration was 0.25 pC/count for this 10 bit system. Several channels were significantly different than this.

## 3 Test Beam Data

Measurements were done for a selected sample of points on the grid of intersections of positive and negative strips. A total of 78 strips were selected for beam studies based on limited running time, our ability to position the strip intersection points in the beam and performance of necessary checks to qualify the data. We performed pedestal measurements for channels whose strips were not in the beam during beam spills. A typical set of pedestal subtracted histograms for the six channels with beam for strips +38 and -38 is shown in Fig. 2.

The triggers for the data shown in Fig.2 depend only on the beam counters shown in Fig. 1. None of the scintillator strips are included in the trigger. This allows for an independent measurement of the efficiency of any strip through which the beam is passing. For the plot shown there are 11,450 events. A careful examination of the six plots shows that there are no events with a pulse height near zero. If there were a single event missing the inefficiency would be  $1/11450 = 8.7 \text{ E-}05$ . Assuming Poisson statistics this inefficiency, implies the mean number of photo-electrons is  $> 9$ . With this simple analysis the mean number of photo-electrons from light pulses produced at the far end of a strip would decrease the efficiency to about 99%, which seems tolerable since strip wrapping, etc. will introduce inefficiencies of a few percent.

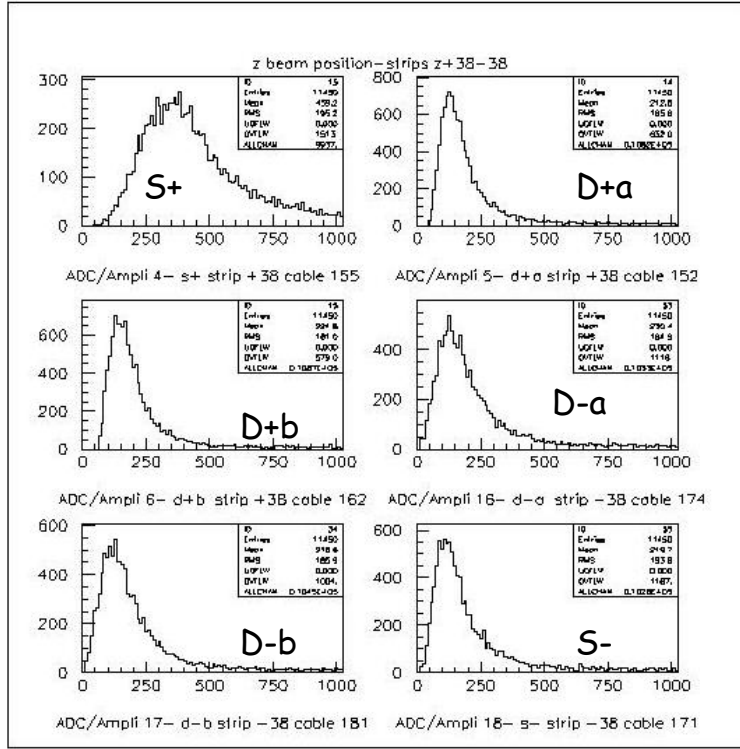


**Figure 2: Pulse height histograms for beam exposure of the four strips centered on the four planes: +38 and -38.**

Another observation from Fig. 2 is that the mean pulse height for these six channels is quite varied. This comes primarily from the different responses of the multi-anode cells to light pulses. Other factors that affect the observed pulse-height distributions from different PMT channels, include the ADC calibration (# of pC/ADC count), variations in the X10 amplifiers, and the light transmission through the thermally-fused splice joint between the clear and WLS fibers. The latter, ~80%, has been measured for each of the 384 fiber splices but it has not been applied in our analysis.

## 4 Measurement of MAPMT Relative Response

There are various schemes that can be used to measure the response of each MAPMT channel. We used a custom setup that mimics green light generated in strips. It is a piece of scintillator that has two 1.01 m long, 1.2 mm diameter Kuraray Y11 fibers embedded in it, with a 5 mCi Sr-90 source (with housing) placed on top of it to produce light pulses. A precision-drilled template with 64 1.2mm diameter holes was used to accurately position the free end of the WLS fiber adjacent to the Hamamatsu 7546B MAPMT photocathode window. The assembled PMT with base voltage divider circuit, cables, and light source were operated in a light-tight box. The output of the MAPMT channel that was illuminated was carried from the light-tight box to a commercial electrometer connected via commercial DAQ apparatus to a PC. One of the two WLS fibers was connected to a given channel for monitoring purposes throughout the measurements[2].

Each of six MAPMTs had their relative response measured with the HV set to 800V. At this voltage the typical current was ~1  $\mu$ A. We also measured cross-talk, i.e. the output of physically adjacent channels when light was incident on one channel. The cross-talk varied from a maximum of 4.9% to an average of 3.9% for the four nearest channels to 1% for the next nearest channels. There was no saturation in the output of any channel as the voltage was varied between 600V and 970V as evidenced by a linear dependence of the logarithm of the current as a function of the voltage. The variation in response over six MAPMTs that were measured is substantial. For all tubes measured the maximum to minimum output varied by a roughly a factor of 5. The mechanical structure of the

MAPMT is reflected in a periodic variation in the relative output over the 64 channels[2].

## 5 Test Results

Figure 3. shows the calibrated response of several channels in pC as a function of distance from beam intersection with a particular strip to the WLS-to-clear splice joint. Included are the ADC calibration and the MAPMT channel's relative response as described by A. Dyshkant et al [2]. The data show that when both ends are readout the summed signal is larger by 30 – 50% than that of a strip with single ended readout.

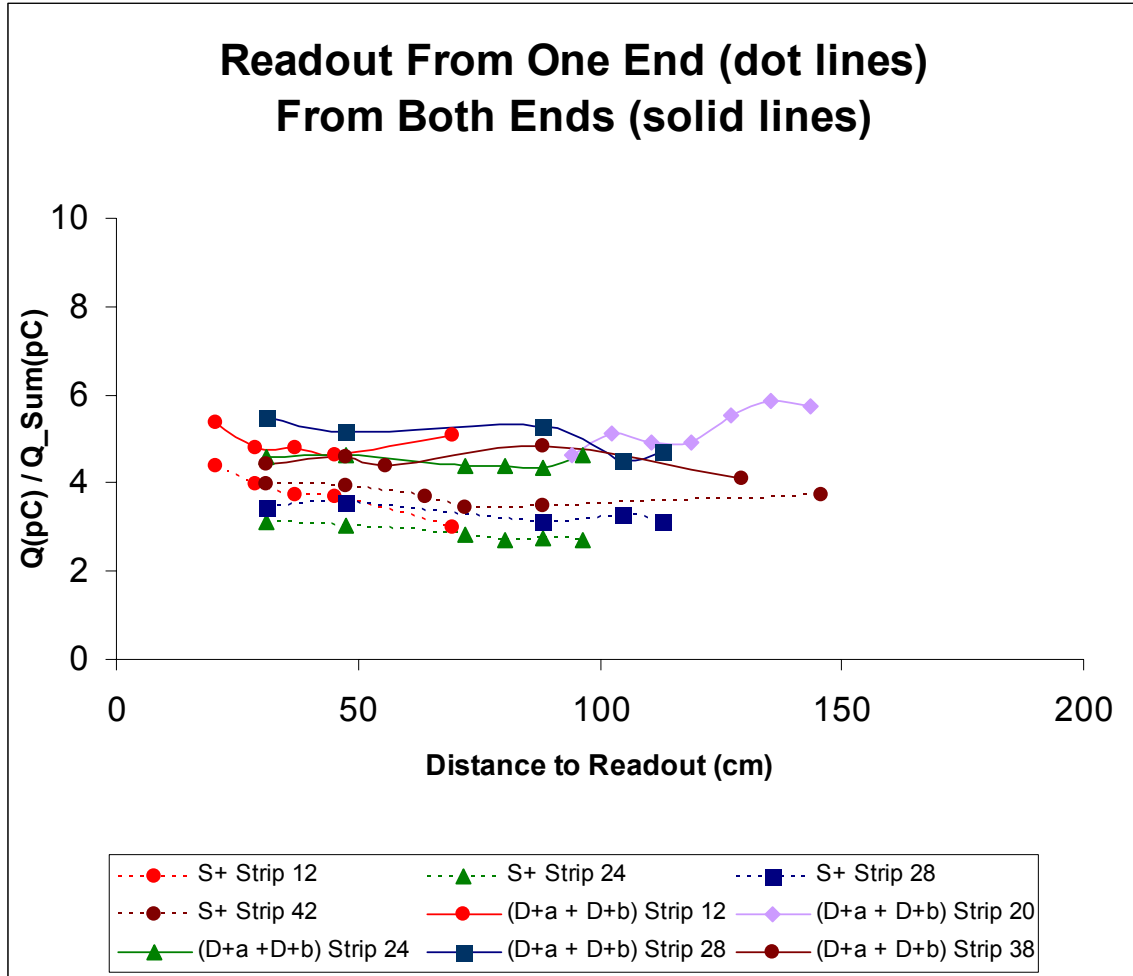


**Figure 3: Signals from scintillator strips after corrections for relative response of different MAPMT channels. The data points connected by dashed (solid) lines are for strips with single-ended (double-ended) readout.**

This is about what was expected based on the attenuation length for green light in the WLS fiber and the reflection coefficient for the mirrored surface that was sputtered on the polished far end of each WLS fiber of the S-planes.

## 6 Testing Si Photo-sensors

Near the end of our MTest running the Udine group attached a few of their IRST photo-sensors [3] to strips that were essentially the same as those tested with MAPMTs. Their installation at the test beam was relatively simple as we were able to attach them on the front face of our movable array of four MAPMT planes. The outputs of the photo-sensors were sent to X10 amplifiers and then to ADCs for digitization. An example of the digitized output is shown in Figure 4 below.

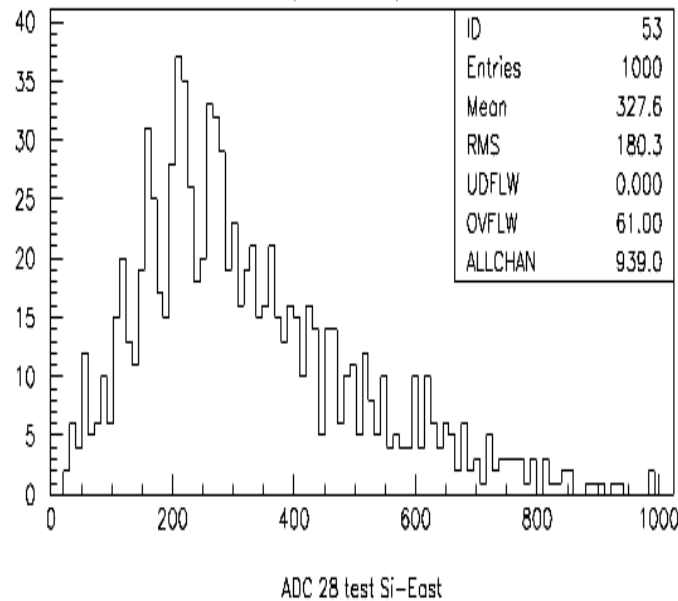


**Figure 4: Test results from an IRST photo-sensor optically coupled to a WLS fiber embedded in a extruded scintillator bar.**

Individual photo-electron peaks are clearly visible. The beam was primarily 120 GeV/c protons with the intensity similar to running with the MAPMT tests. Discriminator thresholds were set above electronic noise but below the single photo-electron amplitude; the dark count did not exceed 1.5 KHz. Data were taken with a trigger based only on beam line scintillation counters as were used in the MAPMT tests. The Si photo-sensor gain is estimated to be  $1.6 \times 10^6$ ; the efficiency is 99% and the mean number of photo-electrons is  $\sim 6.5$ .

## 7 References

- [1] Slides: <http://ilcagenda.linearcollider.org/contributionDisplay.py?contribId=509&sessionId=108&confId=1296>
- [2] A.Dyshkant, G.Blazey, K.Francis, D.Hedin, V.Zutshi, H.E..Fisk, et al, MAPMT H7546B Anode Current Response Study for ILC SiD Muon System Prototype, FERMILAB-PUB-07-485-E, Fermilab (2007).
- [3] C. Piemonte, et al IRST-INFN Trieste/Udine <http://www.sipm.itc.it>